Supplementary Information For

Localization and characterisation of brown rot in two types of acetylated wood

Andrea Ponzecchi[1*], Gry Alfredsen[2], Maria Fredriksson[3], Emil E. Thybring[1], Lisbeth G. Thygesen[1]

[1]Bioresource Chemistry and Technology, Department of Geoscience and Natural Resource Management, University of Copenhagen, Frederiksberg, Denmark
[2]Department of Wood Technology, Norwegian Institute of Bioeconomy Research, Ås, Norway
[3]Division of Building Materials, Lund University, Lund, Sweden

[*]Corresponding author
email : apo@ign.ku.dk
phone: +45 31121040
ORCID: 0009-0009-1654-6458

Table S1 Degree of acetylation (R_{mod}), mass loss, and week of harvest of the samples employed for attenuated total reflectance Fourier transform infrared spectroscopy (ATR-FTIR) and Raman micro-spectroscopy (Raman)

Material	**R_{mod} (g/g)**		**Mass Loss (%)**		**Week of Harvest (weeks)**	
Method	**ATR-FTIR**	**Raman**	**ATR-FTIR**	**Raman**	**ATR-FTIR**	**Raman**
Untreated	0	0	0	0	-	-
	0	0	-1.4	-1.4 ± 0.8	1	0.5 (4 days)
	0	0	9.3	14.9 ± 1.2	4	3 ± 1
	0	0	22.9	31.3 ± 2.6	4	6
Uniform high	0.220	0.223 ± 0.007	0	0	-	-
	0.220	0.223 ± 0.005	14.4	33.6 ± 8.6	33	42
Uniform low	0.149	0.151 ± 0.003	0	0	-	-
	0.165	0.159 ± 0.002	15.9	23.9 ± 7.4	14	15
Interface	0.096	0.108 ± 0.007	0	0	-	-
	0.095	0.097 ± 0.003	29.7	34.9 ± 7.5	14	15

Table S2 Detailed description of: wavenumber range in which peak features (height, area) have been evaluated, spectral range in which the spectrum has been linearly baselined (in addition to the signal pre-processing), wavenumber of the peak of interest followed by the molecular group and structural component, associated with the peak for all the Raman peaks analysed in the study

Peak range [peak center] (cm^{-1})	**Baseline range (cm^{-1})**	**Literature (cm^{-1})**		**Component**
332-415 [380]	330-706	384	C-O-C bend (out of plane) and $O_{(6)}$-H bending[1,2]	Cellulose (crystalline)
578-706 [641]		632	O-C=in-plane deformation[3,4]	hemicellulose, lignin, chelated iron ions, acetylation
865-955	707-1208	910	H-C=C and H-C=O bending[4,5]	hemicellulose, lignin, acetylation
mean (1096,1110)		1095	COC stretching[1,6]	Cellulose (oriented), hemicellulose
max (1129-1142)		1124	COC stretching[1,6]	cellulose, hemicellulose
max (1358-1377)	1208-1529	1376	CH bending[1,6,7]	cellulose, hemicellulose, deuterium oxide in amorphous cellulose
1441-1498		1457	C-H bend of OCH_3 and CH_2[6–9]	lignin, cellulose, chelated calcium ions
1601	1545-1780	1601	aromatic C=C stretch[1,7,8,10]	Lignin aromatic ring
1644-1710		1660	C=C stretch of coniferyl alcohol and C=O stretch of coniferyl aldehyde[1,6,7]	Lignin aliphatic chain
1710-1780		1738	C=O carbonyl stretch[4,11]	acetylation, lignin
2300-2685	2300-2685	2490	O-D stretching[12,13]	water, accessible hydroxyls
mean (2898-2902)	2894-2940	2895	C-H stretch[1,2,5,9,14]	lignin, cellulose, hemicellulose
2941		2942	C=O carbonyl stretching and C-H stretch[1,2,5,7–9,14]	lignin, cellulose, hemicellulose, acetylation
3150-3650	3150-3650	3450	O-H stretching[5]	inaccessible hydroxyls

1. Gierlinger N, Keplinger T, Harrington M, Schwanninger M. Raman Imaging of Lignocellulosic Feedstock. *Cellul - Biomass Convers*. Published online 2013. doi:10.5772/50878.
2. Makarem M, Lee CM, Kafle K, et al. *Probing Cellulose Structures with Vibrational Spectroscopy*. Vol 26. Springer Netherlands; 2019. doi:10.1007/s10570-018-2199-z
3. Bock P. The vibrations of lignin A discussion of the IR and Raman spectra of G-lignins and model compounds. Published online 2020.
4. Digaitis R, Thybring EE, Thygesen LG, Fredriksson M. Targeted acetylation of wood: a tool for tuning wood-water interactions. *Cellulose*. 2021;28(12):8009-8025. doi:10.1007/s10570-021-04033-z
5. Wiley JH, Atalla RH. Band assignments in the raman spectra of celluloses. *Carbohydr Res*. 1987;160(C):113-129. doi:10.1016/0008-6215(87)80306-3
6. Agarwal UP, Ralph SA. FT-Raman spectroscopy of wood: Identifying contributions of lignin and carbohydrate polymers in the spectrum of black spruce (Picea mariana). *Appl Spectrosc*. 1997;51(11):1648-1655. doi:10.1366/0003702971939316
7. Himmelsbach DS, Akin DE. Near-Infrared Fourier-Transform Raman Spectroscopy of Flax (Linum usitatissimum L.) Stems. *J Agric Food Chem*. 1998;46(3):991-998. doi:10.1021/jf970656k
8. Bock P, Gierlinger N. Infrared and Raman spectra of lignin substructures: Coniferyl alcohol, abietin, and coniferyl aldehyde. *J Raman Spectrosc*. 2019;50(6):778-792. doi:10.1002/jrs.5588
9. Bock P, Nousiainen P, Elder T, et al. Infrared and Raman spectra of lignin substructures: Dibenzodioxocin. *J Raman Spectrosc*. 2020;51(3):422-431. doi:10.1002/jrs.5808
10. Agarwal UP. Analysis of cellulose and lignocellulose materials by raman spectroscopy: A review of the current status. *Molecules*. 2019;24(9). doi:10.3390/molecules24091659
11. Adebajo MO, Frost RL, Kloprogge JT, Kokot S. Raman spectroscopic investigation of acetylation of raw cotton. *Spectrochim Acta - Part A Mol Biomol Spectrosc*. 2006;64(2):448-453. doi:10.1016/j.saa.2005.07.045
12. Hofstetter K, Hinterstoisser B, Salmén L. Moisture uptake in native cellulose - The roles of different hydrogen bonds: A dynamic FT-IR study using Deuterium exchange. *Cellulose*. 2006;13(2):131-145. doi:10.1007/s10570-006-9055-2
13. Ponzecchi A, Thybring EE, Fredriksson M, Solsona SP, Thygesen LG. Raman micro-spectroscopy of two types of acetylated Norway spruce wood at controlled relative humidity. 2022;(September):1-9. doi:10.3389/fpls.2022.986578
14. Agarwal UP, Atalla RH. Chapter 4: Vibrational spectroscopy. In: Heitner C, Dimmel DR, Schmidt JA, eds. *Lignin and Lignans: Advances in Chemistry*. 1st ed. CRC Press; 2010:104-136.

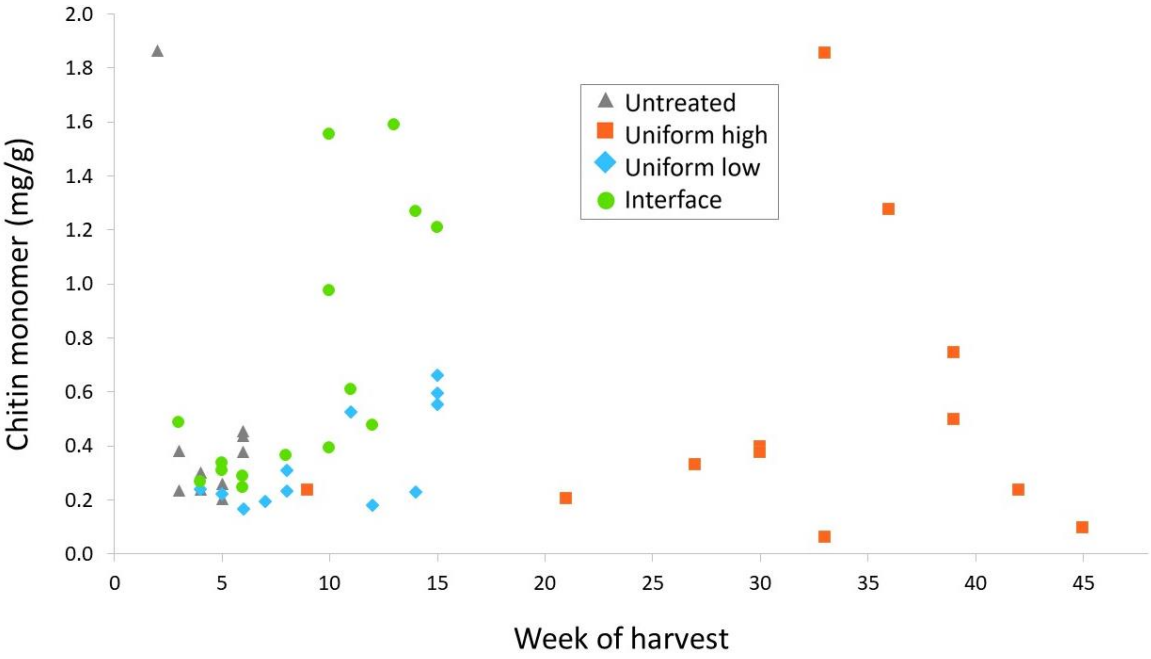

Fig. S1 Chitin monomer content (mg/g) plotted against the week of harvest (week) of selected samples.

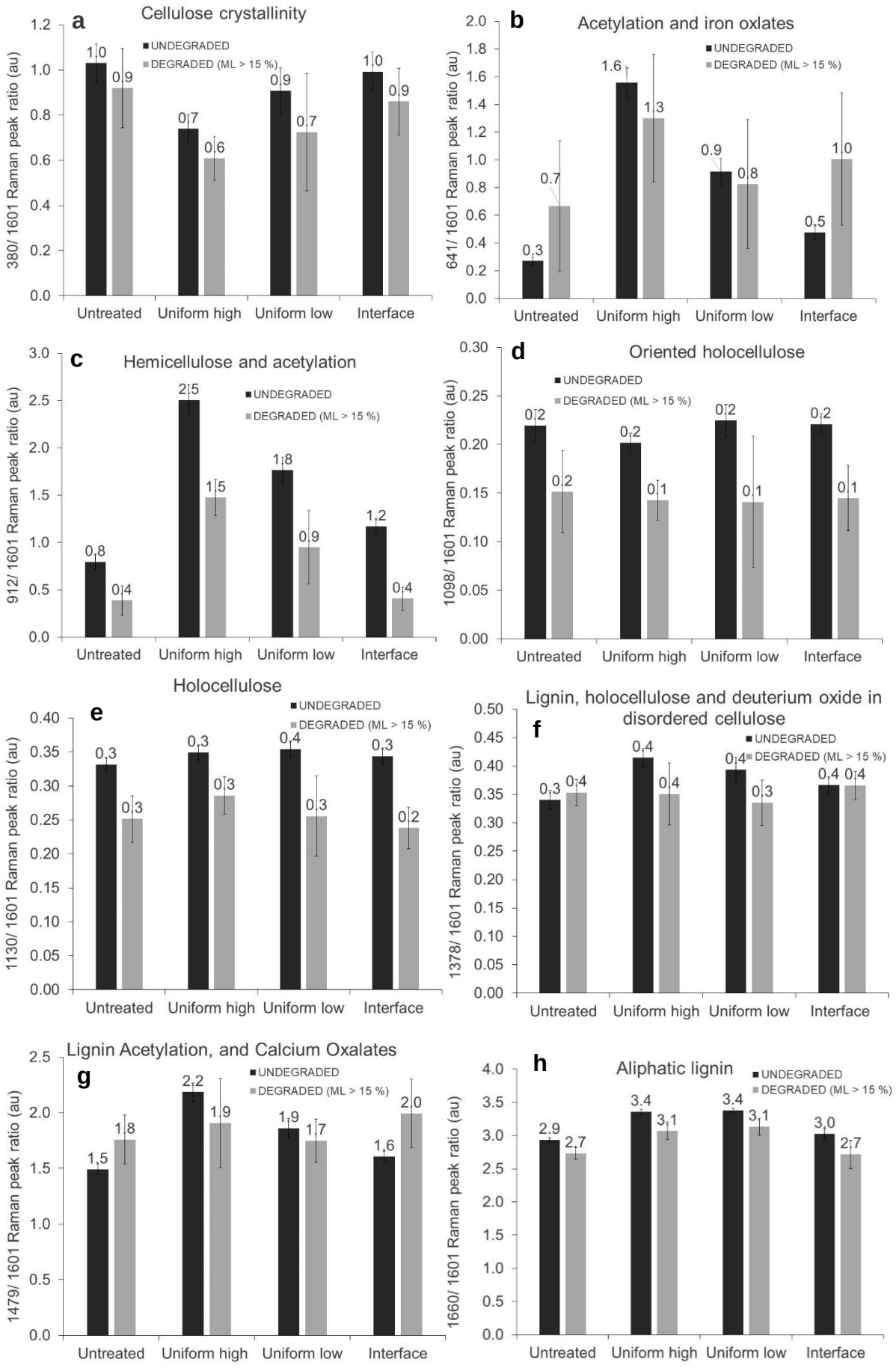
a
Cellulose crystallinity
380/ 1601 Raman peak ratio (au)
UNDEGRADED
DEGRADED (ML > 15 %)
1.0
0.9
0.7
0.6
0.9
0.7
1.0
0.9
Untreated
Uniform high
Uniform low
Interface
b
Acetylation and iron oxlates
641/ 1601 Raman peak ratio (au)
0.3
0.7
1.6
1.3
0.9
0.8
0.5
1.0
c
Hemicellulose and acetylation
912/ 1601 Raman peak ratio (au)
0.8
0.4
2.5
1.5
1.8
0.9
1.2
0.4
d
Oriented holocellulose
1098/ 1601 Raman peak ratio (au)
0.2
0.2
0.2
0.1
0.2
0.1
0.2
0.1
e
Holocellulose
1130/ 1601 Raman peak ratio (au)
0.3
0.3
0.3
0.3
0.4
0.3
0.3
0.2
f
Lignin, holocellulose and deuterium oxide in disordered cellulose
1378/ 1601 Raman peak ratio (au)
0.3
0.4
0.4
0.4
0.4
0.3
0.4
0.4
g
Lignin Acetylation, and Calcium Oxalates
1479/ 1601 Raman peak ratio (au)
1.5
1.8
2.2
1.9
1.9
1.7
1.6
2.0
h
Aliphatic lignin
1660/ 1601 Raman peak ratio (au)
2.9
2.7
3.4
3.1
3.4
3.1
3.0
2.7

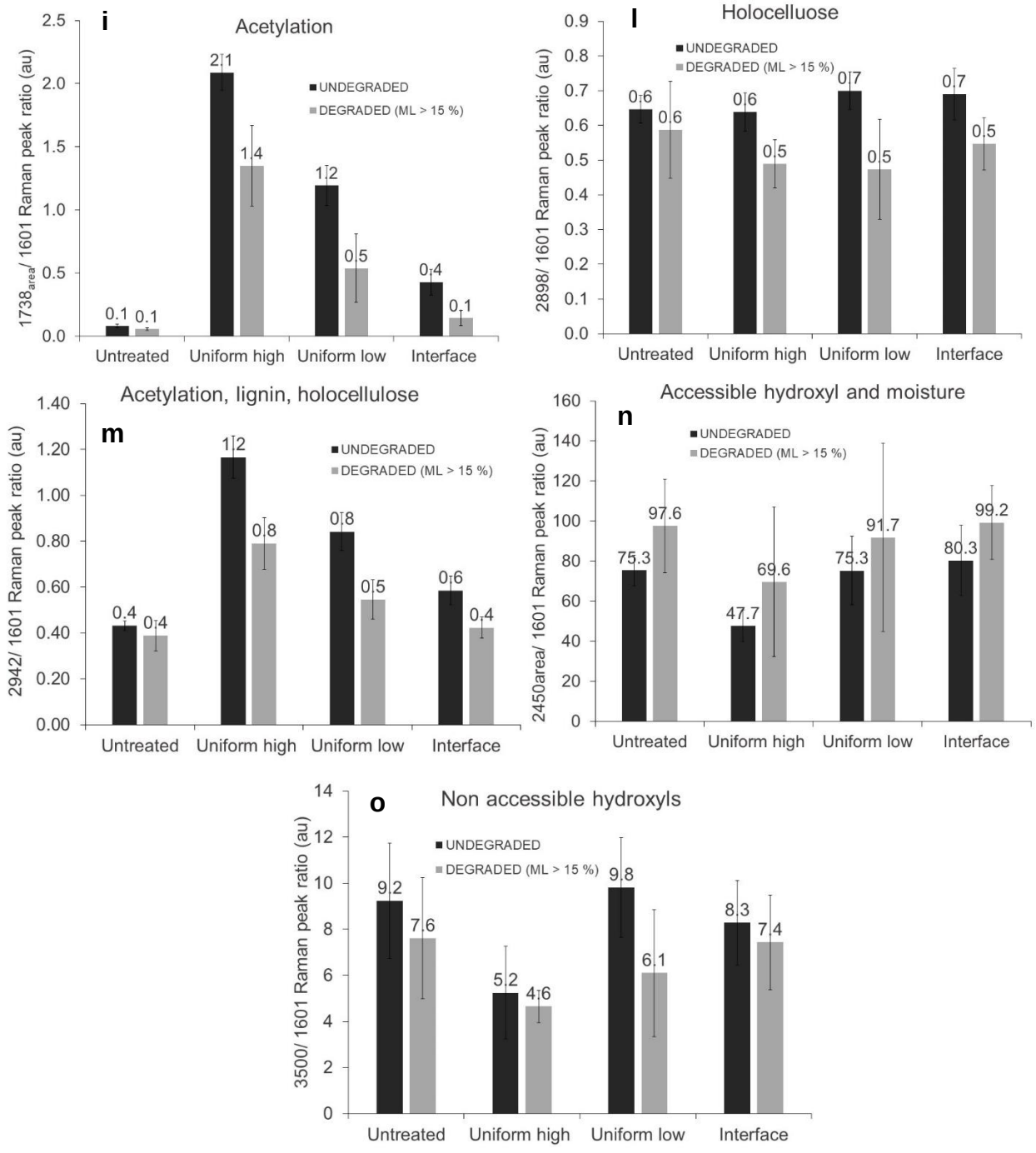

Fig. S2 Bar chart of Raman microspectroscopy intensity maps peak ratios of the average cell wall values of untreated and acetylated samples before and after degradation at different wavenumbers. Number and error bars on the bars represent the mean and the standard deviation of the Raman peak ratio among the six replicates of cell wall tracheids scanned for each type of wood and degradation state

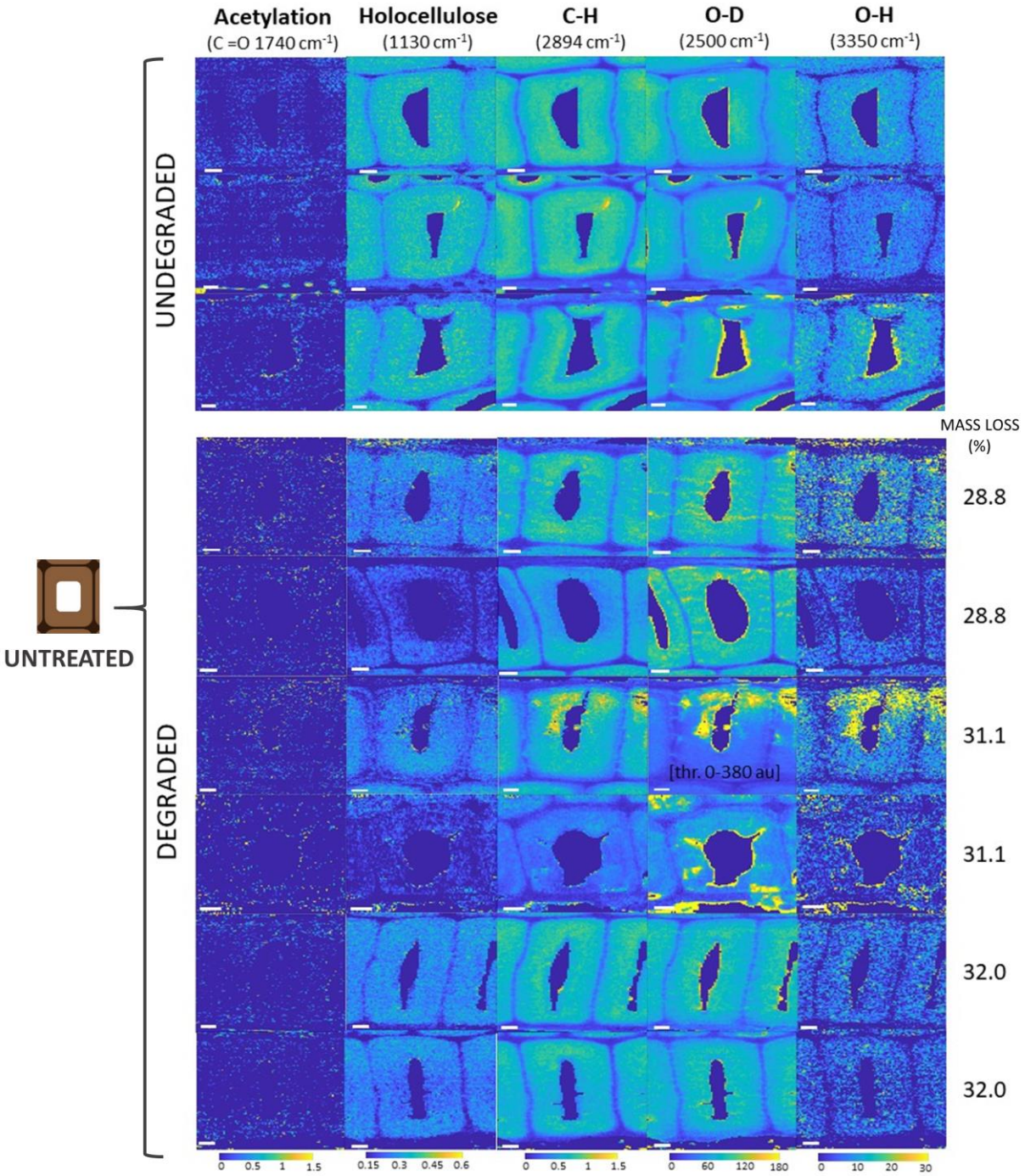

Fig. S3 Overview of Raman microspectroscopy intensity maps of UNTREATED spruce wood cell walls before and after brown rot degradation. The vibrational bond of the maps is described at the top of each columns, while the colour bar is indicated at the bottom. Maps belonging to the same column describe the same vibrational bond and share the same threshold bar. Cell lumina are set to zero. Maps belonging to the same raw describe different vibrational bond of the same tracheid. White scale bar is 5 µm. The text in the third row of degraded samples indicate the adjusted threshold for that specific intensity map

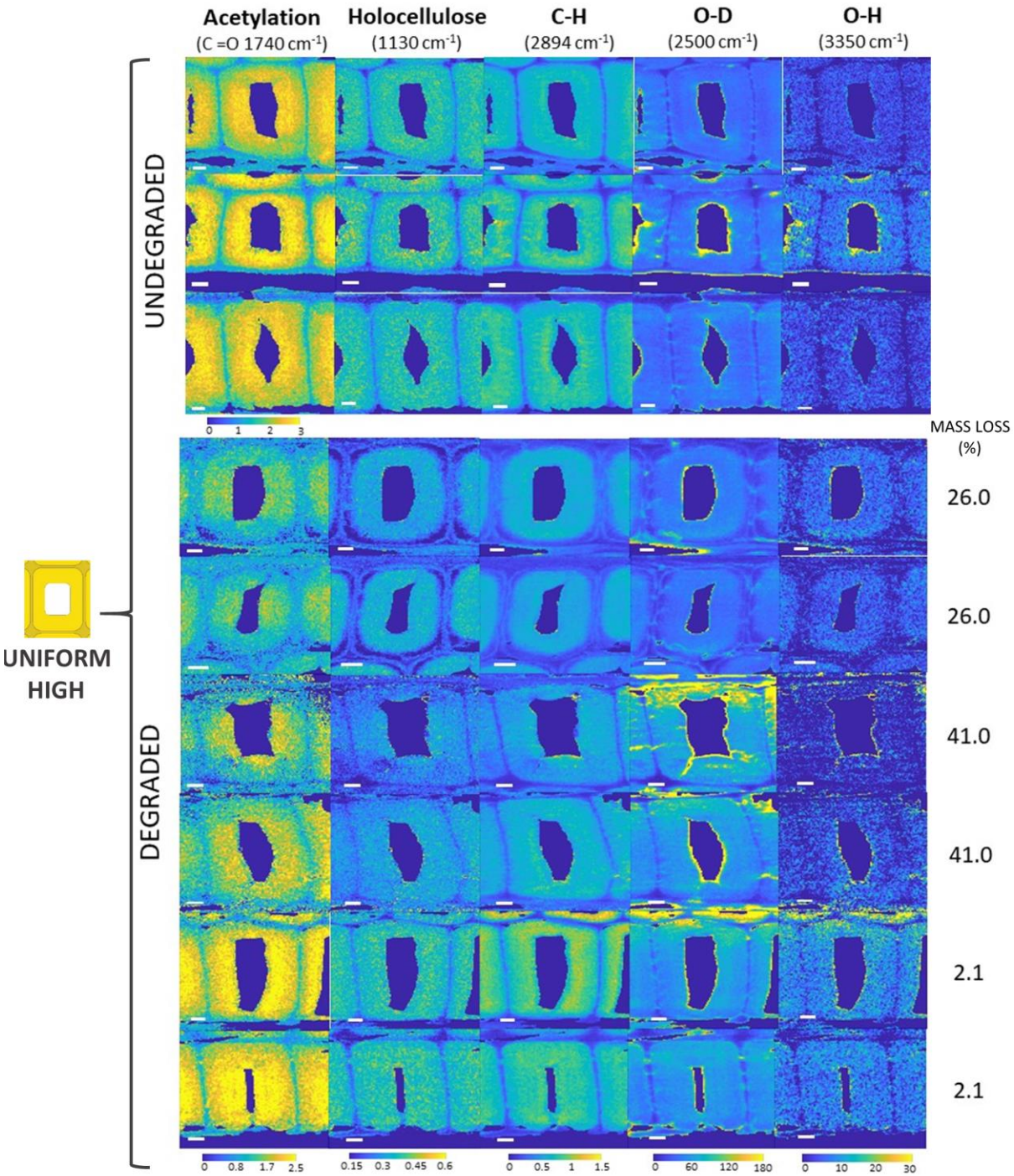

Fig. S4 Overview of Raman microspectroscopy intensity maps of UNIFORM HIGH spruce wood cell walls before and after brown rot degradation. The vibrational bond of the maps is described at the top of each columns, while the colour bar is indicated at the bottom. Maps belonging to the same column describe the same vibrational bond and share the same threshold bar. Cell lumina are set to zero. Maps belonging to the same row describe different vibrational bond of the same tracheid. White scale bar is 5 µm

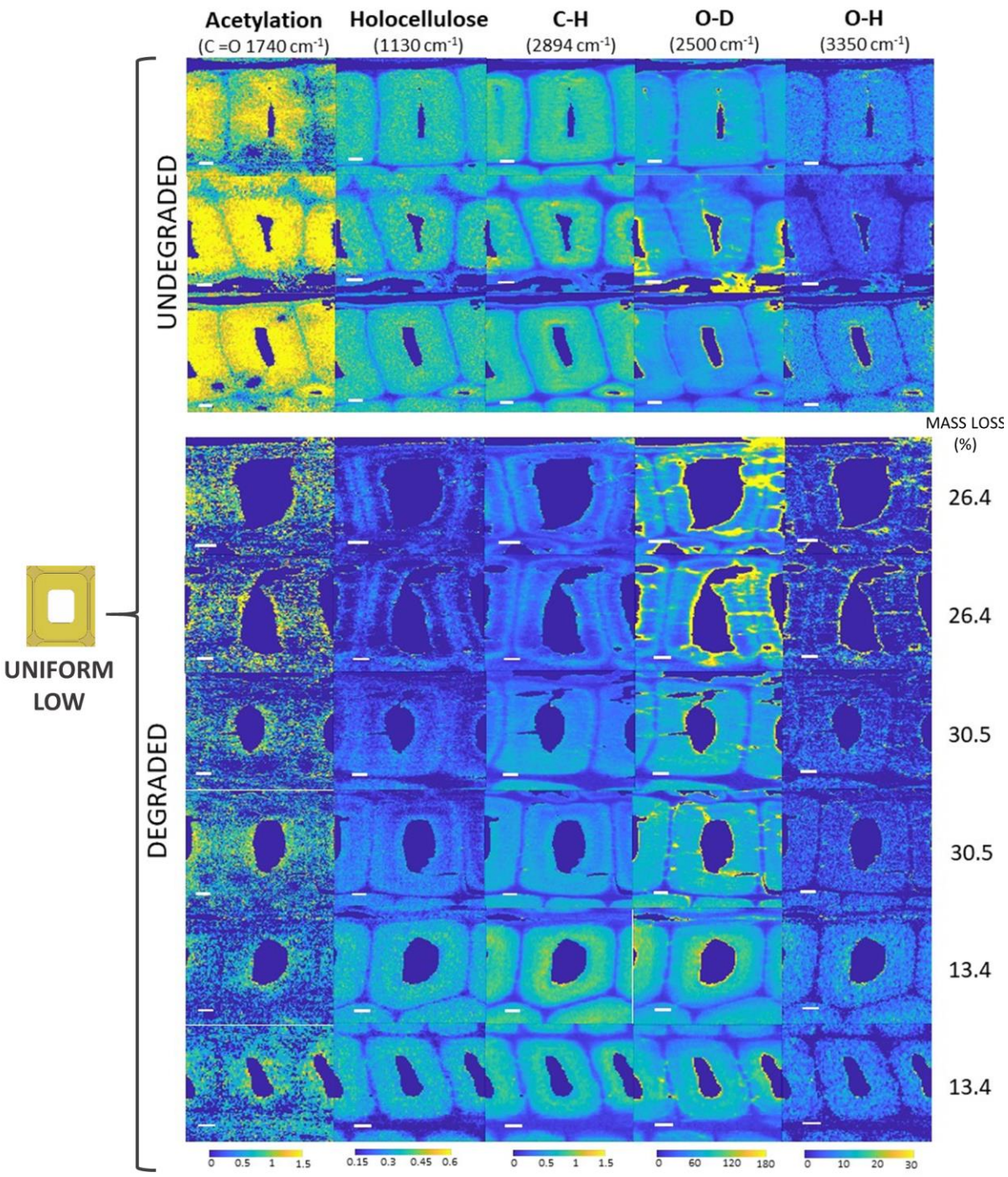

Fig. S5 Overview of Raman microspectroscopy intensity maps of UNIFORM LOW spruce wood cell walls before and after brown rot degradation. The vibrational bond of the maps is described at the top of each columns, while the colour bar is indicated at the bottom. Maps belonging to the same column describe the same vibrational bond and share the same threshold bar. Cell lumina are set to zero. Maps belonging to the same raw describe different vibrational bond of the same tracheid. White scale bar is 5 µm

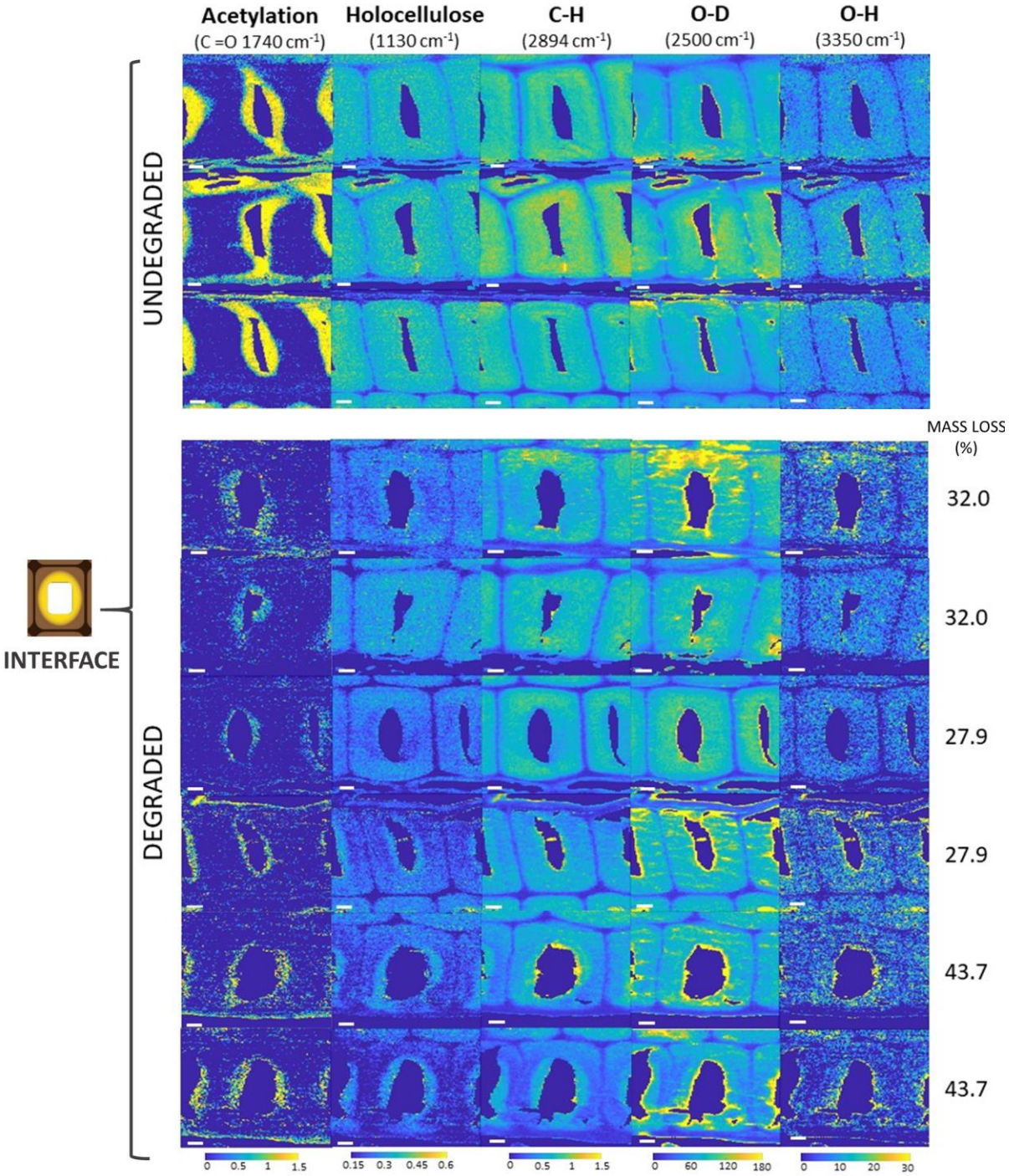

Fig. S6 Overview of Raman microspectroscopy intensity maps of INTERFACE spruce wood cell walls before and after brown rot degradation. The vibrational bond of the maps is described at the top of each columns, while the colour bar is indicated at the bottom. Cell lumina are set to zero. Maps belonging to the same column describe the same vibrational bond and share the same threshold bar. Maps belonging to the same raw describe different vibrational bond of the same tracheid. White scale bar is 5 µm

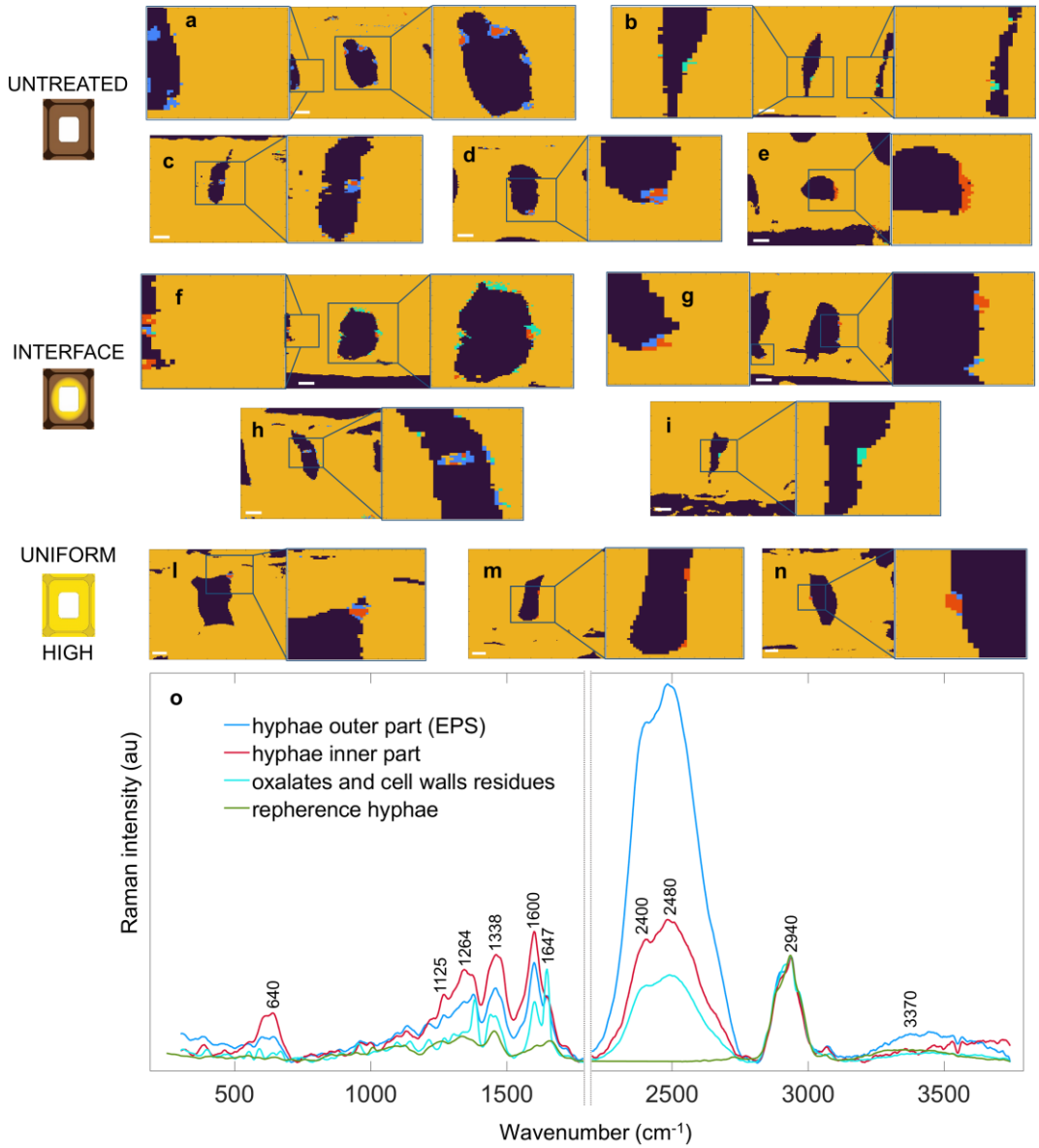

Fig. S7 a-n) Cluster maps of Norway spruce cell wall cross sections after brown rot degradation showing cell wall material in mustard color, lumen in dark blue, while in red and blue the hypothesized hyphae. o-p) Raman spectra of the cluster tentatively assigned to hyphae cell wall and the extracellular polymeric matrix (EPS), reference Raman spectrum of hyphae from *Rhodonia placenta* (Füchtner et al., 2023), and the cell wall/ calcium oxalates residues (light blue), plotted in the wave number region between 320 cm^{-1} and 1780 cm^{-1} (o), and 2190 cm^{-1} and 3750 cm^{-1} (p)